

## Sedimentation profiles of charged colloids: Entropic lift and charge separation

A.-P. HYNINEN<sup>1</sup>, R. VAN ROIJ<sup>2</sup> and M. DIJKSTRA<sup>1</sup>

<sup>1</sup> *Debye Institute, Soft Condensed Matter, Utrecht University  
Princetonplein 5, 3584 CC Utrecht, The Netherlands*

<sup>2</sup> *Institute for Theoretical Physics, Utrecht University  
Leuvenlaan 4, 3584 CE Utrecht, The Netherlands*

(received 31 October 2003; accepted in final form 5 January 2004)

PACS. 82.70.Dd – Colloids.

PACS. 05.20.Jj – Statistical mechanics of classical fluids.

PACS. 61.20.Ja – Computer simulation of liquid structure.

**Abstract.** – We present Molecular Dynamics simulations and Poisson-Boltzmann theory of sedimentation equilibrium of suspensions of charged colloids, treated at the level of the primitive model, including the co- and counterions (microions) explicitly. The simulations provide the first direct confirmation of the theoretical low-salt predictions of i) a macroscopic separation of colloidal and microionic charge, ii) an almost homogeneous electric field in the suspension, iii) a highly non-barometric colloid density distribution. These effects, which cannot be explained within the usual effective one-component picture, should be measurable experimentally.

*Introduction.* – Colloidal suspensions are multi-component fluids that consist of mesoscopic colloidal particles in a molecular solvent, often with additional components such as ions, polymers, etc. Despite this multicomponent character, it is common practice to view a colloidal suspension as an effective one-component system of colloidal particles [1, 2]. In this letter we study sedimentation of suspensions of charged colloids in the Earth's gravity field, and show that the resulting equilibrium density profile can only be understood in terms of macroscopic charge separation of colloids and salt ions, *i.e.* the effective one-component description breaks down.

Colloidal suspensions exhibit sedimentation in the Earth's gravity field when the buoyant mass  $m$  of the colloidal particles is non-vanishing [3, 4]. The equilibrium colloid density  $\rho(z)$  at height  $z$  follows, within a one-component picture, from the competition between minimal energy (all colloids at  $z = 0$ , *i.e.* at the bottom) and maximum entropy (a homogeneous distribution in the available volume). For a dilute suspension at temperature  $T$ , the equilibrium density profile satisfies the well-known barometric height distribution

$$\rho(z) = \rho_0 \exp[-z/L], \quad (1)$$

with  $L = k_{\text{B}}T/mg$  the gravitational length in terms of the Boltzmann constant  $k_{\text{B}}$  and the gravitational acceleration  $g$  [5]. The normalization constant  $\rho_0$ , which is the number density

at  $z = 0$ , follows from the total number  $N = A \int_0^H dz \rho(z)$  of colloids in the system, where  $A$  is the planar area and  $H$  the height of the sample. Of course, the colloidal interactions affect the competition between potential energy and entropy, and hence change the functional form of  $\rho(z)$ , but one would expect that  $L$  sets the length scale for the sedimentation equilibrium in dilute suspensions. Typically,  $L$  is of the order of  $\mu\text{m}$ – $\text{mm}$  for colloids, unless density matching has taken place by special preparation of the sample.

There is, however, both theoretical [6–10] and experimental [11] evidence that  $L$  is *not* necessarily the relevant length scale in suspensions of highly charged colloids at low ionic strength. The reason is that the usual competition between potential (gravitational) energy and colloid entropy is enriched by two additional free-energy contributions in such systems, i) the entropy of the microscopic ions (which favors the cations and anions to be homogeneously distributed in the sample), and ii) the electrostatic energy (which favors local charge neutrality). At low enough concentrations of salt these two contributions are in conflict with eq. (1) when  $L \ll H$ : in order to satisfy local charge neutrality the counterion distribution must, in the absence of an appreciable number of coions, also be of the form (1), *i.e.* the counterion distribution will be extremely inhomogeneous on the length scale of the sample size  $H$ . (At sufficiently high-salt concentrations the relative ion fractionation is much smaller.) How does the system resolve this conflict? Theoretical treatments of this problem have so far all been based on Poisson-Boltzmann (mean-field) theory, which predicts that the system sets up an almost homogeneous macroscopic electric field in the suspension (*i.e.* in a conducting medium!), such that the colloids are lifted to heights of order  $QL$ , with  $Q > 0$  the colloidal charge number that can easily be  $10^2$ – $10^4$  experimentally. In order to assess the possibility of experimental observation of this intriguing phenomenon, important questions are whether or not the predictions are i) robust with respect to approximations of the theory (which ignores fluctuations, correlations, and hard-core excluded-volume effects), and ii) quantitatively reliable. In this letter we present, for the first time, the results of a computer simulation study of this system, and put the mean-field theory, in particular the version of ref. [10], to the test directly. We briefly present the theory first for completeness. For more details, the reader is referred to ref. [10].

*Theory.* – We consider a suspension of  $N$  colloidal spheres of charge  $Qe$  (with  $e$  the proton charge,  $Q > 0$ ) and gravitational length  $L$ , in a structureless solvent with dielectric constant  $\epsilon$  at temperature  $T$ , in osmotic contact with a salt reservoir with a concentration  $2\rho_s$  of monovalent cations and anions. The ions are massless, and their (yet unknown) average equilibrium density profile in the suspension can be written as a Boltzmann distribution  $\rho_{\pm}(z) = \rho_s \exp[\mp\phi(z)]$  [10]. Here  $\phi(z)$  is the yet unknown dimensionless electrostatic (Donnan) potential, which follows with the equilibrium colloid density profile  $\rho(z)$  from the combined Boltzmann distribution and Poisson-Boltzmann equation,

$$\begin{cases} \rho(z) &= \rho_0 \exp[-z/L - Q\phi(z)], \\ \phi''(z) &= -4\pi\lambda_B(Q\rho(z) - 2\rho_s \sinh \phi(z)), \end{cases} \quad (2)$$

subject to the boundary conditions  $\phi'(0) = \phi'(H) = 0$ . Here  $\lambda_B = e^2/\epsilon k_B T$  is the Bjerrum length, and a prime denotes differentiation with respect to  $z$  [10]. Below, we solve this set of equations numerically for the parameters of the simulation. However, this set of equations, or variations thereof, was already studied in refs. [6, 7, 9, 10], and was found to have solutions  $\phi(z)$  linear in  $z$  in a macroscopically large volume provided the ion concentration is so low that  $2\rho_s \ll Q^2\rho(z)$ . In the salt-free case, the resulting electric field is such that the electric force on a colloidal particle is  $mgQ/(Q+1)$ , which with a gravitational force of  $-mg$  yields a

net force  $-mg/(Q+1)$ , *i.e.* as if the mass were reduced by a factor  $Q+1$ . Hence the colloidal distribution is much more homogeneous than predicted by the barometric law (1), and the typical height of the sediment is now  $(Q+1)L$  instead of  $L$  [6, 7, 9, 10]. In the limit of high salt,  $2\rho_s \gg Q^2\rho(z)$ , the barometric law (1) is recovered.

We wish to stress that the present theoretical description is entirely of mean-field nature, and disregards *any* of the correlations, *i.e.* correlations are not even accounted for on the Debye-Hückel level. For a homogeneous system of charged particles (which is obtained here when  $m = 0$ ) this level of approximation leads trivially to an ideal-gas mixture in a spatially constant Donnan potential, but in the gravity-induced inhomogeneous system of present interest non-trivial phenomena already show up within this low-level description.

*Simulation method.* – We perform Molecular Dynamics (MD) simulations in a box of dimensions  $K \times K \times H$ , taken periodic in the horizontal directions  $x, y \in [0, K]$  and finite in the vertical direction  $z \in [0, H]$ . We consider  $N$  colloids of positive charge  $Qe$  and diameter  $\sigma$ ,  $N_+$  coions of charge  $+e$ , and  $N_- = QN + N_+$  counterions of charge  $-e$ . The microions have a (small) diameter in order to prevent the system from collapsing. Since a hard-core repulsion is not well-suited for MD simulations, we replace it, following ref. [12], by a softer  $r^{-9}$  potential, such that the pair potential between particles of species  $i$  and  $j$  (*i.e.* between colloid-colloid, colloid-microion, and microion-microion pairs) is given by

$$U_{ij}(r) = k_B T \frac{Q_i Q_j \lambda_B}{r} + k_B T \frac{|Q_i Q_j| \lambda_B}{9} \left( \frac{\sigma_i + \sigma_j}{2} \right)^8 \frac{1}{r^9}, \quad (3)$$

where  $Q_i$ ,  $\sigma_i$  is the valency and diameter of species  $i$ , respectively, while  $r = |\mathbf{r}_i - \mathbf{r}_j|$ . The prefactor of the soft repulsion was chosen such that the potential well of oppositely charged particles is located at hard-core contact,  $r = (\sigma_i + \sigma_j)/2$  [12]. In addition to the pair interaction in eq. (3), the colloids are coupled to the gravitational field that points in the negative  $z$ -direction, and the potential is given by  $V(z) = k_B T z/L$  with  $L$  the gravitational length defined earlier. The microions are considered massless, and do not couple to the gravitational field.

The long range of the Coulomb interaction requires the use of periodic images to account for the electrostatics properly. The standard Ewald summation method [13] cannot be used, since the system is only periodic in the  $x$ - and  $y$ -, and *not* in the  $z$ -direction. Instead we employed the so-called MMM2D method, which can deal with the slab geometry of present interest properly and efficiently [14, 15]. In order to keep the particles inside the simulation box, repulsive walls are added at  $z = 0$  and  $z = H$ . The wall potential for species  $j$  is given by the soft  $r^{-9}$  repulsion of eq. (3), now with  $r$  equal to the distance from the wall and  $i$  equal to the macroion species. This choice mimics, to a good approximation, a hard wall with contact distance given by  $(\sigma + \sigma_j)/2$ .

It is important to note that the simulated system is *not* osmotically coupled to a salt reservoir; the number of microions is fixed. In principle, this complicates the direct comparison with the theory presented earlier [10], where the reservoir salt concentration is fixed and *not* the actual concentration in the suspension. However, we see that the top part of the simulation box contains such a low colloid density that it acts as a reservoir, and the measured total salt concentration in the top can be directly identified with the reservoir salt concentration  $2\rho_s$ .

The MD simulations are performed for fixed particle numbers, volume, and temperature. Constant temperature is achieved by using the so-called Langevin dynamics [16], where the equation of motion for each particle is a Langevin equation instead of the usual Newton equation (that gives rise to a constant energy). Denoting the potential energy of a configuration by  $U$ , the Langevin equation for particle  $i$  at position  $\mathbf{r}_i(t)$  at time  $t$  can be written as [16]

$$m_i \ddot{\mathbf{r}}_i = -\nabla_i U - \nu m_i \dot{\mathbf{r}}_i + \mathbf{F}_i(t), \quad (4)$$

where  $m_i$  is the inertial mass of the particle,  $\nu$  a friction coefficient,  $\mathbf{F}_i(t)$  a random force, and the dots denote time derivatives. The dissipative term,  $-\nu m_i \dot{\mathbf{r}}_i$ , damps the motion of the particles, while the fluctuating term,  $\mathbf{F}_i(t)$ , gives particles random pushes and therefore, on average, accelerates the motion of the particles. Together these two terms provide a heat bath at constant temperature, provided the fluctuation-dissipation theorem is satisfied by setting  $\langle \mathbf{F}_i(t) \rangle = 0$  and  $\langle \mathbf{F}_i(0) \cdot \mathbf{F}_i(t) \rangle = 2m_i k_B T \nu \delta(t)$ , where the brackets denote the average over a Gaussian distribution. We use the velocity Verlet algorithm to integrate eq. (4) [16], and employ reduced units: the colloid diameter  $\sigma$  and mass  $m$  are the units of length and mass, respectively, and  $k_B T$  is the unit of energy, resulting in  $\sigma \sqrt{m/k_B T}$  for the unit of time.

The density profiles  $\rho(z)$ ,  $\rho_+(z)$  and  $\rho_-(z)$  for the macro- and microions are calculated from the particle configurations recorded during a simulation run. The electric field  $E(z)$  along the  $z$ -axis inside the simulation box is calculated from the integrated Poisson equation, that in dimensionless form is given by

$$\mathcal{E}(z) = \frac{\sigma e E(z)}{k_B T} = -4\pi \frac{\lambda_B}{\sigma} \sigma^2 \int_0^z q(z') dz', \quad (5)$$

where  $q(z) = Q\rho(z) + \rho_+(z) - \rho_-(z)$  is the total charge density. One can directly compare the simulated  $\mathcal{E}(z)$  with the theoretical prediction  $\sigma\phi'(z)$  that follows from the solution of eq. (2).

*Results.* – In all four simulations (labeled (a)-(d)) presented here we set  $\lambda_B = 4 \times 10^{-3} \sigma$ , the inertial mass of the microions  $0.01m$ ,  $L = 10\sigma$ , the lateral dimension of the box  $K \approx 7.24\sigma$ , and the total colloidal packing fraction  $\eta = (\pi/6)\sigma^3 N/AH = 0.01$ . The height of the box is  $H = 100\sigma$ , except in (d), where  $H = 50\sigma$ . Simulations (a) and (b) represent salt-free systems ( $N_+ = 0$ ) of  $N = 100$  colloids, where  $Q = 10$  and  $N_- = 1000$  in (a) and  $Q = 5$  and  $N_- = 500$  in (b). Simulations (c) and (d) have added salt, with (c) having  $N = 100$  colloids and  $N_+ = 250$  added coions and (d)  $N = 50$  colloids and  $N_+ = 625$  added coions. In simulations (a)-(c) we use microion diameter  $\sigma_{\text{ion}} = 10^{-3}\sigma$  and in (d) we use  $\sigma_{\text{ion}} = 0.01\sigma$ . The friction coefficient in the Langevin equation (4) is chosen to be  $\nu = 5 \times 10^{-5}/\Delta t$  for all simulations, and the time step for the velocity Verlet algorithm is chosen to be  $\Delta t = 1 \times 10^{-4} \sigma \sqrt{m/k_B T}$  for (a)-(c) and  $\Delta t = 5 \times 10^{-5} \sigma \sqrt{m/k_B T}$  for (d). Such a small  $\Delta t$  requires long simulations to properly sample the colloidal degrees of freedom.

The colloidal charges  $Q = 5$  and  $Q = 10$  that we use are much lower than is typical of realistic colloidal suspensions, where  $Q = 10^2$ – $10^4$ . Such a low colloidal charge is used here for practical reasons: it keeps the total number of particles in the system low enough and the colloid-ion interaction weak enough for fast and efficient simulations [12], while the mechanisms at work can yet be revealed. Note that  $\lambda_B/\sigma$  and  $\sigma_{\text{ion}}/\sigma$  do have values that are typical of colloidal suspensions.

The salt-free simulations (a) and (b) were started with colloids and ions distributed homogeneously and randomly in the simulation box, while the added-salt simulations (c) and (d) had an initial distribution that approximately corresponds to the theoretical prediction [10]. In all cases, the density profiles  $\rho(z)$  were only acquired after carefully checking that the averaged center of mass of the colloids had reached a plateau, indicating that the sedimentation equilibrium had been reached. In order to check the consistency of our methods, simulations (a) and (b) were first performed without electrostatic interactions and, as expected, the barometric height distribution of eq. (1) was recovered at large enough heights.

In fig. 1 we plot the simulated density profiles  $\rho(z)$  together with the corresponding theoretical predictions (the smooth curves) based on numerical solutions of eq. (2). The inset of fig. 1 shows the corresponding microion density profiles. In the theoretical calculation for (c) and (d) we used reservoir salt concentrations  $\rho_s = 0.08/\sigma^3$  and  $\rho_s = 0.285/\sigma^3$ , respectively;

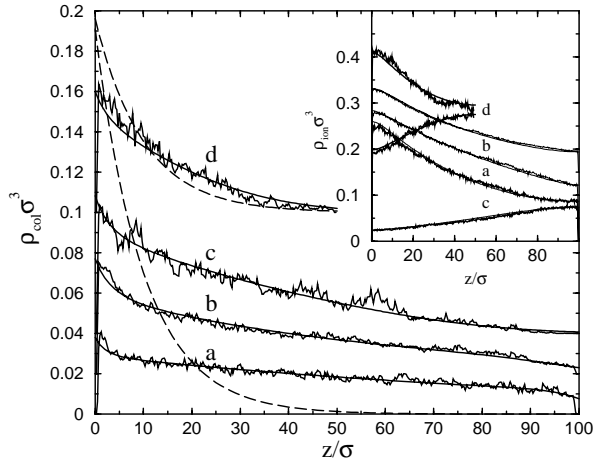


Fig. 1 – Density profiles  $\rho(z)$  for a colloidal suspension of height  $H = 100\sigma$ , total packing fraction  $\eta = 0.01$ , Bjerrum length  $\lambda_B = 4 \times 10^{-3}\sigma$ , and gravitational length  $L = 10\sigma$ , with colloidal charge number  $Q$  given by (a)  $Q = 10$  without added salt, (b)  $Q = 5$  without added salt, and (c)  $Q = 5$  with  $N_+ = 250$  added cations. The curves labeled (d) correspond to  $H = 50\sigma$ ,  $Q = 5$  and  $N_+ = 625$  added cations. For clarity, the colloid density profiles for (b), (c) and (d) are shifted upwards by  $0.02\sigma^3$ ,  $0.04\sigma^3$  and  $0.1\sigma^3$ , respectively. The inset shows the corresponding microion density profiles where the density profile for (b) is shifted upwards by  $0.15\sigma^3$ . The smooth solid curves are the theoretical Poisson-Boltzmann predictions based on eq. (2) and ref. [10], and the dashed curves give the barometric density distributions with  $L = 10\sigma$  for both  $H = 100\sigma$  and  $H = 50\sigma$ .

these values were obtained from (an extrapolation of) the simulated co- and counterion densities in the top of the container. Figure 1 shows that in all four cases the simulation results for both the colloid and ion density profiles agree almost quantitatively with the theoretical

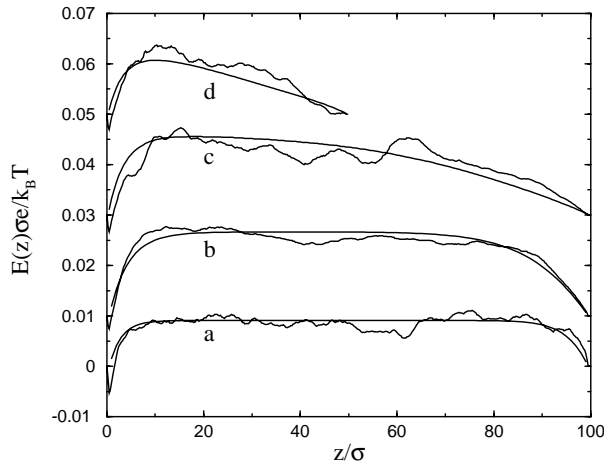


Fig. 2 – Simulated dimensionless electric field  $\mathcal{E}(z)$  defined in eq. (5) and its theoretical prediction  $\sigma\phi'(z)$  (smooth curve) for the parameter choices (a)-(d) as in fig. 1. For clarity, the graphs for (b), (c) and (d) are shifted upwards by  $0.01\sigma e/k_B T$ ,  $0.03\sigma e/k_B T$  and  $0.05\sigma e/k_B T$ , respectively.

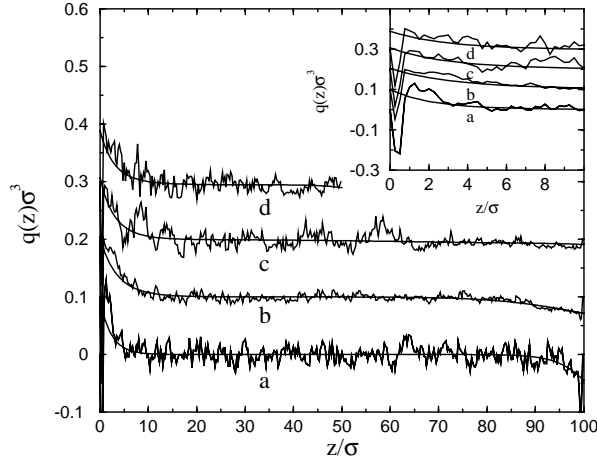


Fig. 3 – Total charge density profile  $q(z)$  showing a positive charge at the bottom and a negative charge at the top, for systems (a)-(d) labeled as in fig. 1. The inset shows a close-up of the bottom region (see text). The smooth curves represent the theoretical predictions. For clarity, the graphs for (b), (c) (d) are shifted upwards by  $0.1\sigma^3$ ,  $0.2\sigma^3$  and  $0.3\sigma^3$ , respectively.

estimates. Note that the simulation data for the added-salt cases (c) and (d) are noisier than in the salt-free cases (a) and (b). The relatively poor statistics in (c) and (d) is due to the larger number of particles in these systems, which require a longer simulation CPU time. The dashed curves in fig. 1 represent the colloidal barometric height distributions of eq. (1) with  $L = 10\sigma$ . As can be clearly seen, the density profiles (a)-(c) are far from being barometric, while the profile for the high-salt system (d) is close to the barometric distribution.

The non-barometric distributions are due to a spontaneously formed electric field, which we plot in fig. 2. Again, it is seen that the agreement between the simulation results and the theory is remarkable. The non-zero electric field inside the container is caused by charge separation between the colloids and the microions. In other words, there is excess positive charge from the colloids at the bottom of the box and, conversely, excess negative charge from the microions at the top. The charge separation is readily observed in fig. 3, where we plot the total charge density  $q(z)$ . In systems (a)-(c) there are clearly two peaks in the total charge density, one at the bottom ( $z = 0\sigma$ ) and one at the top ( $z = 100\sigma$ ) of the box. In fact, as is seen from the inset in fig. 3 where we show a close-up of the bottom region of the simulation box, there is also another negative peak at the bottom which is caused by the exclusion of the colloids from the bottom wall due to their size. This “fine structure” of the peak is *not* accounted for in the present version of the theory, as it ignores the finite colloidal size. It can, however, be included and explain the exclusion effect.

*Conclusions.* – We show, for the first time by simulation, that a non-density-matched colloidal suspension in a gravitational field gives rise to a macroscopic charge separation of colloids and microions, provided the added-salt concentration is low enough (but *not* necessarily unphysically low). The mechanism, which was already identified in earlier work [4,6–10], is due to the intricate balance between colloidal and ionic entropy, potential energy, and electrostatic energy. The electric field that is generated by the charge separation is shown to be almost constant in the suspension, and is such that it largely compensates the gravitational force on the colloids, so that the colloids are lifted to altitudes much larger than their gravitational

length. This implies that the system cannot be understood as an effective one-component system of colloids, not even at rather low densities [10].

Our simulations agree quantitatively with the Poisson-Boltzmann theory of ref. [10], which we briefly repeated here, *i.e.* the (mean-field) theory is robust with respect to the inclusion of fluctuations, correlations, and hard-core effects present in the simulations. We note that the low Coulomb coupling of the present system is large enough to induce the entropic lift mechanism, but is yet small enough to ignore correlations in the theory. Given that the four systems presented here span the whole interval from the low- (zero-) salt regime close to the high-salt regime, and that the predictions of the theory hold quantitatively for the rather low colloidal charges considered here, it is tempting to conclude that the theoretical prediction of the entropic lift of the colloids due to a macroscopic electric field may also be rather accurate, or at least qualitatively correct, for low-salt suspensions of highly charged colloids. We hope that this motivates more experimental studies of the sedimentation equilibrium of charged colloids.

\* \* \*

This work is part of the research program of the “Stichting voor Fundamenteel Onderzoek der Materie (FOM)”, which is financially supported by the “Nederlandse Organisatie voor Wetenschappelijk Onderzoek (NWO)”. We thank the Dutch National Computer Facilities foundation for access to the SGI Origin 3800 and SGI Altix 3700. The High Performance Computing group of Utrecht University is gratefully acknowledged for ample computer time.

## REFERENCES

- [1] DERJAGUIN B. and LANDAU L., *Acta Physicochim. URSS*, **14** (1941) 633.
- [2] VERWEY E. J. W. and OVERBEEK J. TH. G., *Theory of the Stability of Lyotropic Colloids* (Elsevier, Amsterdam) 1948.
- [3] VRIJ A., *J. Chem. Phys.*, **72** (1980) 3735.
- [4] PIAZZA R., BELLINI T. and DEGIORGIO V., *Phys. Rev. Lett.*, **71** (1993) 4267.
- [5] BIBEN T., HANSEN J.-P. and BARRAT J.-L., *J. Chem. Phys.*, **98** (1993) 7330.
- [6] BIBEN T. and HANSEN J.-P., *J. Phys. Condens. Matter*, **6** (1994) A345.
- [7] SIMONIN J.-P., *J. Phys. Chem.*, **99** (1995) 1577.
- [8] LÖWEN H., *J. Phys. Condens. Matter*, **10** (1998) L479.
- [9] TÉLLEZ G. and BIBEN T., *Eur. Phys. J. E*, **2** (2000) 137.
- [10] VAN ROIJ R., *J. Phys. Condens. Matter*, **15** (2003) 53569.
- [11] PHILIPSE A. P. and KOENDERINK G. H., *Adv. Colloid Interface Sci.*, **100-102** (2003) 613.
- [12] LOBASKIN V. and LINSE P., *J. Chem. Phys.*, **111** (1999) 4300.
- [13] FRENKEL D. and SMIT B., *Understanding Molecular Simulations*, 2nd edition (Academic Press) 2002.
- [14] ARNOLD A. and HOLM C., *Chem. Phys. Lett.*, **354** (2002) 324.
- [15] ARNOLD A. and HOLM C., *Comput. Phys. Commun.*, **148** (2002) 327.
- [16] ALLEN M. P. and TILDESLEY D. J., *Computer Simulation of Liquids* (Clarendon Press, Oxford) 2002.